THE JOURNAL OF PHYSICAL CHEMISTRY B

 VOLUME 106, NUMBER 46, NOVEMBER 21, 2002

ARTICLES

Self-Diffusion in Two- and Three-Dimensional Powders of Anisotropic Domains: An NMR Study of the Diffusion of Water in Cellulose and Starch

Daniel Topgaard* and Olle Söderman

Division of Physical Chemistry 1, Center for Chemistry and Chemical Engineering, Lund University, P.O. Box 124, S-221 00 Lund, Sweden

Received: January 16, 2002; In Final Form: August 1, 2002

The pulsed field gradient stimulated echo NMR technique is applied to the study of water diffusion in biological porous materials (a sheet of wood cellulose fibers and a packed bed of potato starch granules) consisting of randomly oriented domains with an anisotropic supermolecular organization. Expressions are presented for the probability distribution of apparent diffusion coefficients due to two- and three-dimensional powder distributions of domain orientations. The distributions are converted to echo attenuation curves with a method taking cross relaxation between the water and the solid matrix into account. Using a model in agreement with the structure and domain orientation known from other experimental techniques, it is found that the mean diffusion coefficient and degree of anisotropy (ratio between water diffusivity parallel and perpendicular to the structure director) at a level of hydration corresponding to approximately 90% relative humidity are (1.68 ± 0.03) $\times 10^{-11}$ m^2/s and 6.4 ± 0.9 for cellulose and (7.8 ± 0.1) $\times 10^{-12}$ m^2/s and 2.5 ± 0.3 for starch, respectively. A systematic examination of different models for the diffusion coefficient distribution shows that the chosen models are not unique in describing the data. For the estimation of anisotropy, a physically correct model is required. The average diffusion coefficient can be determined with any reasonable model, not necessarily physically correct.

Introduction

NMR diffusometry is a technique well suited for the study of porous materials.[1−4] Information on the porous structure is obtained by following the self-diffusion of probe molecules contained within the porous matrix. Materials with an ordered arrangement of the structural elements may exhibit diffusional anisotropy, e.g., lyotropic liquid crystals,[5−7] starch,[8−10] wood,[11] and pulp fibers.[12] If the material is macroscopically ordered, the result of the diffusion experiment depends on the orientation of the sample relative to the measuring direction as defined by the direction of the magnetic field gradient. Experiments on materials consisting of randomly oriented anisotropic domains, each giving rise to a certain apparent diffusion coefficient, the value of which depends on the orientation relative to the gradient, are traditionally analyzed in terms of a sum of echo attenuation profiles (NMR signal intensity vs the experimental variable *k)*, originating from the individual domains.[8]

Self-diffusion experiments on small amounts of water in biomaterials using the pulsed field gradient stimulated echo (PFG STE) technique are affected by cross relaxation between water and the macromolecular matrix.[13,14] In this case, the classical Stejskal−Tanner equation[15] for echo attenuation is not

* To whom correspondence should be addressed. E-mail: Daniel.Topgaard@fkem1.lu.se. Phone: INT +46 46 222 01 34. Fax: INT +46 46 222 44 13.

10.1021/jp020130p CCC: $22.00
Published on Web 10/25/2002

valid. To analyze PFG spin−echo (PFG SE) experiments on water in wheat starch, Callaghan et al.[8] used the Stejskal−Tanner expression (which is valid for the PFG SE experiment) as a starting point for the derivation of echo attenuation curves for 3D powders of anisotropic objects. The PFG STE technique has a few advantages in comparison with the PFG SE method; for example, it is possible to investigate materials with lower water concentration. Wider ranges of diffusion times are also experimentally accessible. A drawback is that the interpretation of the experimental data is more difficult when cross relaxation is present.

In this paper, we present expressions for the probability distribution of diffusion coefficients originating from 2D and 3D powders of anisotropic domains with cylindrical symmetry. For the case with no cross relaxation, the distributions are converted to echo attenuation profiles via a Laplace transform. Cross relaxation is taken into account by using an integral transform involving an analogue to the Stejskal−Tanner equation which is valid in the presence of cross relaxation. The use of a diffusion coefficient distribution emphasizes that many different distributions and models satisfy the same experimental data, a fact well-known from, e.g., dynamic light scattering[16] and NMR relaxation.[17,18] To extract the relevant information, a physically correct model of the anisotropy with respect to water diffusion must be used.

As a demonstration of the approach, self-diffusion experiments on water sorbed in a paper sheet consisting of cellulose fibers and water in a packed bed of starch granules are analyzed. A paper sheet can be considered as a 2D powder of anisotropic fibers. An approximately spherical starch granule has a radial and tangential organization of the structural elements. A bed of starch granules can thus be regarded as a 3D powder of anisotropic domains. The measured diffusion coefficients and anisotropy can be related to the tortuosity tensor of the water-filled pore space.[19] This property has a practical use in the prediction of water and solute migration through the structure, e.g., in the removal of water from a paper sheet in the drying section of a papermaking machine.

Materials and Methods

The samples used were a paper made of bleached kraft pulp obtained from SCA Research, Sundsvall, Sweden, and potato starch obtained from Lyckeby Stärkelsen, Kristianstad, Sweden. The samples were exposed to humid air at room temperature. The final water content was determined from the free induction decay.[14,20] The water contents correspond to a relative humidity of approximately 90%.

NMR self-diffusion measurements were performed with the PFG STE technique[21] on a Bruker DMX 200 spectrometer equipped with a Bruker gradient probe. The experiment consists of a stimulated echo, $90°-\tau_1-90°-\tau_2-90°-\tau_1-$echo, with one gradient pulse of length δ and strength G in each τ_1 period. The separation between the leading edges of the gradient pulses is $\Delta = \tau_1 + \tau_2$, and the effective diffusion time is $t = \Delta - \delta/3$. For experiments on cellulose, δ was 0.5 ms and τ_1 was 1.1 ms. In the experiments on starch, δ was 2 ms and τ_1 was 3.1 ms. t was varied between 20 and 100 ms in four geometrically spaced steps by changing the delay τ_2. For each value of t the gradient strength was stepped up linearly to the maximum value G_{max}, which was 9.6 T/m for the shortest t. For the longer t, G_{max} was decreased in order to keep tG_{max}^2 constant. The phase of the 90° pulses were cycled according to the procedure suggested in Fauth et al.[22] For the experiments on cellulose, the gradients were directed along the plane of the paper sheet. The echo amplitude was obtained by digitizing the second half of the echo, performing a numerical Fourier transform and finally numerically integrating the frequency domain peak.

Theoretical Considerations

The PFG STE experiment is sensitive to molecular motion along one dimension defined by the direction of the magnetic field gradient. For isotropic Gaussian diffusion of a monodisperse species, the echo amplitude $E(k)$ obeys the Stejskal−Tanner equation[15]

$$E(k) = \exp(-kD) \tag{1}$$

where D is the self-diffusion coefficient and

$$k = (\gamma G\delta)^2(\Delta - \delta/3) \tag{2}$$

where γ is the gyromagnetic ratio of the spin bearing nucleus and the pulse sequence parameters are defined in the Materials and Methods section.

In the presence of cross relaxation the analogue to eq 1 is given by[13,14]

$$E(k) = \exp(-kD)f(k,D,\tau_2,C,k_wk_c) \tag{3}$$

$$f(k,D,\tau_2,C,k_wk_c) = \exp(A\tau_2/2) \times \frac{\cosh(B\tau_2/2) - \frac{A+C}{B}\sinh(B\tau_2/2)}{\cosh(B_0\tau_2/2) - \frac{C}{B_0}\sinh(B_0\tau_2/2)}$$

$$A = kD/(\Delta - \delta/3)$$

$$B = \sqrt{(A+C)^2 + 4k_wk_c}$$

$$B_0 = \sqrt{C^2 + 4k_wk_c}.$$

Cross relaxation is quantified by the parameters C and k_wk_c (see refs 13 and 14 for a definition), which can be determined with the Goldman−Shen experiment.[23]

Consider an object which has a preferential direction of its structural elements, e.g., the pulp fiber in Figure 1a. The (macroscopic) diffusion of water in such an object will depend on the direction of observation. For a material with cylindrical symmetry, the observed diffusion coefficient D_θ depends on the angle θ between the director, i.e., the axis of cylindrical symmetry, and the direction of the magnetic field gradient through[8]

$$D_\theta = D_{||}\cos^2\theta + D_\perp \sin^2\theta \tag{4}$$

where $D_{||}$ and $D_\perp$ are the self-diffusion coefficients parallel and perpendicular to the director. The total signal for a macroscopic sample with many domains, illustrated in Figure 1b, is obtained by integrating the contributions from all of the domains:

$$E(k) = \int_0^{\pi/2} P_\theta(\theta)\exp(-kD_\theta)\mathrm{d}\theta \tag{5}$$

where $P_\theta(\theta)$ is the probability distribution of θ, normalized in the interval $0 < \theta < \pi/2$. For a 2D powder, $P_\theta(\theta) = 2/\pi$, and for a 3D powder, $P_\theta(\theta) = \sin\theta$. Equation 5 was evaluated by Callaghan[8] for the 3D case to

$$E(k) = \exp(-kD_\perp)\int_0^1 \exp[-k(D_{||} - D_\perp)x^2]\,\mathrm{d}x \tag{6}$$

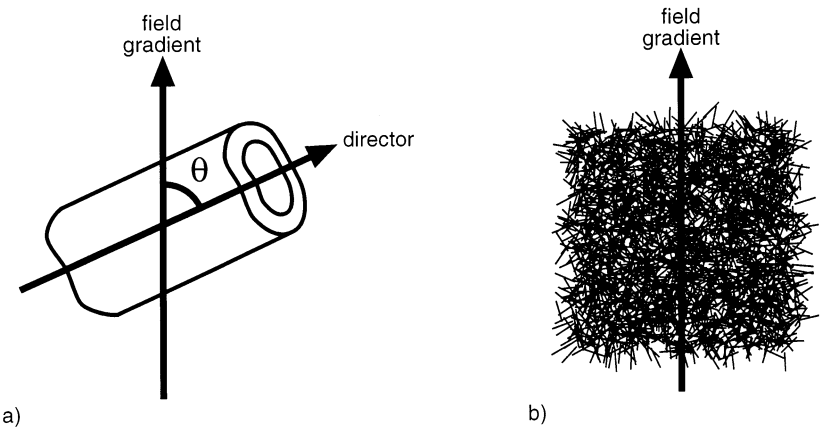

Figure 1. Schematic picture of (a) an anisotropic object and (b) a 2D powder of anisotropic objects. θ is the angle between the structure director and the magnetic field gradient.

No such simple expression can be found in the presence of cross relaxation.

An alternative approach to the summing of echo decays is to reinterpret $P_\theta(\theta)$ as a diffusion coefficient distribution $P_D(D)$ through

$$P_D(D) = \int_0^{\pi/2} P_\theta(\theta)\delta(D - D_\theta)\, d\theta \tag{7}$$

Here, δ denotes the Dirac delta function (not to be confused with the gradient pulse length). The echo attenuation is then calculated by the Laplace transform

$$E(k) = \int_0^\infty P_D(D) \exp(-kD)\, dD \tag{8}$$

For the case with cross relaxation, $\exp(-kD)$ is replaced with eq 3.

A general distribution $P_D(D)$ can be characterized with its mean value $\langle D\rangle$

$$\langle D\rangle = \int_0^\infty DP_D(D)\, dD \tag{9}$$

and the nth moment $\langle D^n\rangle$

$$\langle D^n\rangle = \int_0^\infty (D - \langle D\rangle)^n P_D(D)\, dD \tag{10}$$

For a 2D powder, $\langle D\rangle = (D_\perp + D_\parallel)/2$, and for a 3D powder, $\langle D\rangle = (2D_\perp + D_\parallel)/3$. $\langle D^2\rangle$ is a measure of the width, and $\langle D^3\rangle$ quantifies the asymmetry of the distribution (in a linear sense).

The advantage of using the indirect route via $P_D(D)$, instead of a direct summing of echo attenuation curves, is that comparison between different models is facilitated, both by simple comparison of plots of the different $P_D(D)$ and through calculation of the moments of the distribution. A further advantage is that the relation between $E(k)$ and $P_D(D)$ is well established in the literature, especially in the interpretation of diffusion in multicomponent or polydisperse systems.[24]

To avoid singularities of $P_D(D)$ at $D_\perp$ and $D_\parallel$, the delta-function in eq 7 can be replaced with a smoother function

$$f(D,\theta) = \frac{1}{D\sigma\sqrt{2\pi}} \exp\left[-\frac{1}{2}\left(\frac{\ln(D/D_\theta)}{\sigma} - \sigma\right)^2\right] \tag{11}$$

Equation 11 becomes a delta function in the limit $\sigma \to 0$, is symmetric with respect to log D, and has a maximum value at D_θ. The use of eq 11 has no influence on the echo attenuation curves as long as σ is small (0.02 in our calculations), but the numerical solution of the integrals is facilitated and the visual appearance of a plot of $P_D(D)$ is improved.

Results and Discussion

In this section, we will first present the experimental results for cellulose and interpret the results in terms of a model that is consistent with information from other sources. Subsequently, we will demonstrate the importance of external information by analyzing the data with models that are *not* physically reasonable but, nevertheless, are able to reproduce the experimental data. Finally, the results obtained on starch are presented.

Cellulose. A paper sheet is a network of cellulose fibers. The fiber, several tenths of micrometers wide and some millimeters long, consists of closely packed rodlike cellulose microfibrils, ~10 nm wide and several hundred nanometers long, oriented mainly in the direction of the fiber.[25] Visual inspection of the paper sheet reveals that the individual fibers are almost exclusively oriented in the plane of the sheet and randomly distributed within this plane. Hence, the paper sheet can be considered as a 2D powder of fibers. The preferential orientation of the microfibrils in the direction of the fiber axis leads to faster diffusion parallel to the fiber. The length and thickness of the fiber wall is large enough to neglect end effects leading to restricted diffusion. Furthermore, the persistence length of the fiber is much larger than the typical distance traveled by water during the diffusion time, implying that exchange between sections with different orientations on the experimentally accessible time scale is negligible. The physical object that corresponds to the anisotropic domain is a part of the cellulose fiber with constant orientation, i.e., a segment of the fiber shorter than the persistence length. Because the fibers are randomly distributed within the paper sheet, the sample constitutes a 2D powder of anisotropic domains.

Experimental data from the PFG STE experiment obtained on a paper sample hydrated to 0.15 g water/g cellulose is displayed in Figure 2. The data are shown as a Stejskal−Tanner plot, i.e., E vs k. For a diffusion process characterized by a single and constant value of D, the data would collapse onto a single straight line and D could be extracted from the slope according to eq 1. In this case, changes of t, G, and δ are equivalent, and k is the appropriate variable. Different slopes of E vs k at different values of t is generally interpreted as restricted diffusion or diffusion in a system with fractal dimensionality.[1] We have previously shown that the dependence on t is the result of cross relaxation occurring on the same time scale as the values of t.[14] In this case, there is no convenient variable taking changes

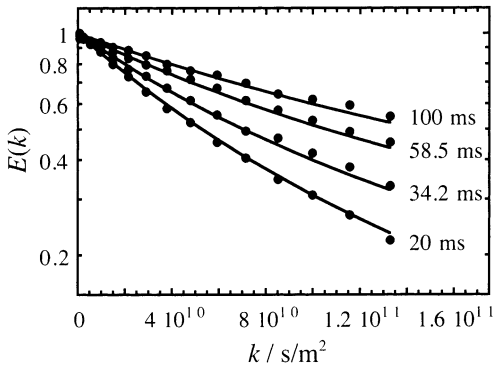

Figure 2. Echo attenuation curves $E(k)$ measured with the PFG STE experiment on a hydrated paper sheet oriented parallel to the gradient. The values of the diffusion time t are indicated in the figure. The water content is 0.15 g water/g solid. Circles, experimental; lines, fit of eq 8 with $\exp(-kD)$ replaced by eq 3 and $P_D(D)$ calculated with eq 7 using $P_\theta(\theta)$ for a 2D powder. $P_D(D)$ is assumed to be independent of t. The different slopes of the curves obtained at different values of t are results of cross relaxation. The parameters quantifying the cross relaxation are determined with an independent experiment and are thus treated as known constants in the fitting procedure.

of t, G, and δ into account. We choose to display the data in the well-established Stejskal−Tanner form, although changes of t and $G\delta$ no longer have equivalent influence on the appearance of the echo profiles.

From the facts presented above, we conclude that the water diffusion along a paper sheet can be analyzed using eq 8 with $\exp(-kD)$ replaced by eq 3 and $P_D(D)$ calculated with eq 7 using $P_\theta(\theta)$ for a 2D powder. The integrals in eqs 7 and 8 were evaluated numerically. The integration limits in eq 8 was sufficiently large for the integrand to have reached zero. The resulting expression was incorporated in a global nonlinear fitting routine using $\langle D\rangle$, $D_\parallel/D_\perp$, and the initial intensities for the curves with different t as adjustable parameters. The values of $\langle D\rangle$ and $D_\parallel/D_\perp$ are thus assumed to be independent of t, which is reasonable considering the known structure and the experimentally accessible range of t. The cross relaxation parameters C and $k_w k_c$ were determined with an independent experiment as described in Topgaard and Söderman.[14] The incorporation of cross relaxation effects does not introduce any more adjustable variables, although it introduces some uncertainty because the parameters describing the cross relaxation must be experimentally determined. The separation between the curves in Figure 2 is a result of cross relaxation which is quantified with an independent experiment. The curvature arises because of the different orientations of the anisotropic domains. Apart from the initial intensities, there are only two adjustable parameters: the mean value and the width of the distribution which correspond to the slope and the curvature of the curves. As can be seen in Figure 2, the echo attenuation curves are well described with the derived expression. To get an estimate of the accuracy of the obtained parameters, a Monte Carlo error estimation[26] was performed. The results of the error analysis are presented as histograms in Figure 3. The parameter determined with greatest accuracy is $\langle D\rangle$, whereas $D_\parallel$, $D_\perp$, and $D_\parallel/D_\perp$ have a wider spread. $\langle D\rangle = (1.68\pm0.03) \times 10^{-11}$ m^2/s and $D_\parallel/D_\perp = 6.4\pm0.9$ with 67% confidence level. $P_D(D)$ calculated with the most likely parameters is shown in Figure 4.

The Importance of Prior Knowledge. It is commonly recognized that distributions obtained through an inverse integral transform of experimental data are extremely sensitive to noise and the choice of method for inversion.[16−18,27,28] The model with

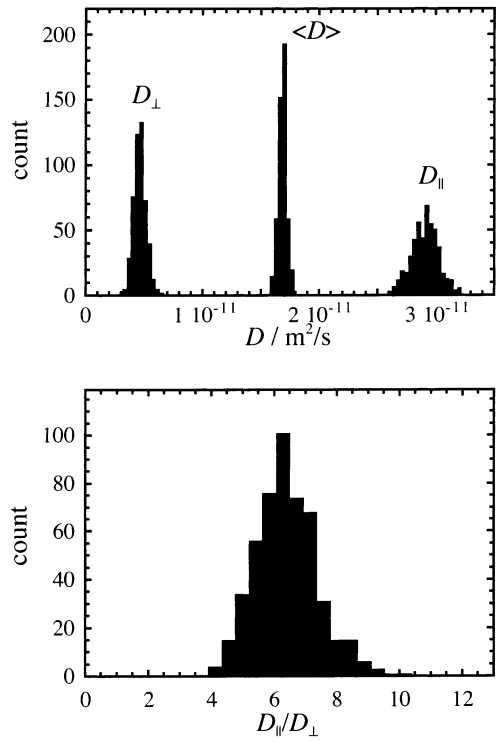

Figure 3. Histograms of parameters from a Monte Carlo estimation of the error in the fit in Figure 2. (a) $D_\perp$, $\langle D\rangle$, and $D_\parallel$ from left to right. (b) Degree of anisotropy $D_\parallel/D_\perp$.

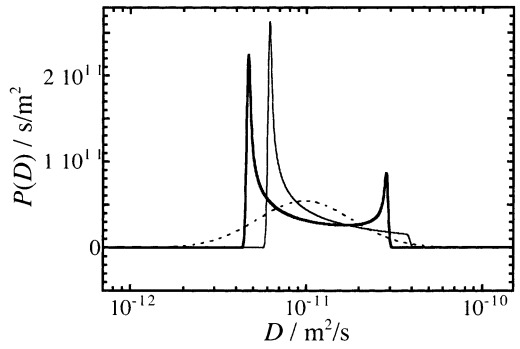

Figure 4. Diffusion coefficient distributions $P_D(D)$ that are consistent with the experimental data in Figure 2. Thick solid line, 2D powder; thin solid line, 3D powder; and thin dashed line, log−normal distribution.

a 2D powder distribution of anisotropic fibers gives a satisfactory description of echo attenuation curves obtained on cellulose. We like to point out that the obtained $P_D(D)$ is by no means unique in describing the experimental data. In Figure 4, we present alternative solutions that give an equally good fit to the data. The Laplace transforms of these three distributions, which give the echo attenuations in the absence of cross relaxation, are displayed in Figure 5. The curves coincide within the first decade of attenuation while disagreement appears at higher attenuation. To experimentally discriminate between the models thus requires extremely high quality data, which is difficult to obtain with NMR diffusion experiments. Prior knowledge about the material is therefore of prime importance in the determination of the best model. Although the distributions look rather dissimilar, they have some features in common which are illustrated in Table 1 where the three first moments of the distributions are summarized. There is a good agreement of the first moments, some similarity of the second moments, and orders of magnitude differences of the third moments. The stability of the different moments with respect to noise in the

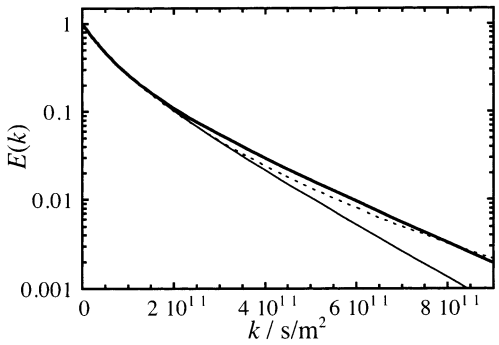

Figure 5. Echo attenuations curves $E(k)$ calculated through a Laplace transform of the diffusion coefficient distributions $P_D(D)$ in Figure 4, neglecting the effect of cross relaxation. The symbols have the same meanings as in Figure 4.

TABLE 1: Moments of the Distributions in Figure 4[a]

	$\langle D\rangle$/ $(10^{-11}$ m^2/s)	$\langle D^2\rangle$/ $(10^{-11}$ m^2/s$)^2$	$\langle D^3\rangle$/ $(10^{-11}$ m^2/s$)^3$
2D powder	1.68 ± 0.03	0.74 ± 0.01	0.016 ± 0.004
3D powder	1.71	0.97	0.61
log−normal	1.74	1.42	4.1

[a] The limits represent 67% confidence level as estimated with a Monte Carlo error analysis.

data was estimated for the model with the 2D powder using the Monte Carlo method. As can be seen in Table 1, the moments are not very sensitive to noise, indicating that the difference in the two higher moments is a result of the model chosen.

From these facts, it can be concluded that an accurate estimate of $\langle D\rangle$ can be obtained with any of the three models. This is important from a pragmatic point of view when there is an interest in how the average tortuosity, which can be calculated from $\langle D\rangle$, changes with some experimental condition, e.g., the relative humidity. In this case, the choice of model can be based on computational convenience. However, when the anisotropy is of interest, the model must give an adequate description of reality.

Starch. The structure and molecular organization of starch granules have been extensively investigated with various microscopic techniques.[29] The granule is of more or less distorted spherical shape and has a diameter of tenths of micrometers. Alternating crystalline and semicrystalline layers, a few hundred nanometers thick, form concentric shells centered around the hilum. Amorphous channels extend in the radial direction throughout the structure.

Displacements on the micrometer scale are detected with PFG STE diffusion measurements on water sorbed in starch granules. This implies that the effect of structures on the hundred nanometer scale is averaged. The size of the granule is large enough to neglect the effects of restricted diffusion, at least to a first approximation. The tangential and radial organization makes it probable that water diffusion in the two directions are different. Because of the structural complexity, in contrast to the microfibril alignment in the direction of the cellulose fiber, it is not evident in what direction the diffusion should be faster. A cone extending in the radial direction from the center of the spherical granule can be considered as an anisotropic domain. Water close to the granule center is more likely to experience domains with different orientations. With increasing t, the fraction with such averaged behavior will increase and the observed anisotropy will decrease. However, the amount of water at a certain distance from the granule center scales with the distance squared, implying that the signal is dominated by the anisotropically mobile water located away from the center. It is uncertain whether a decrease of anisotropy will be detectable before the effect of restricted diffusion is dominant. This regime of t is beyond experimental access with the present system.

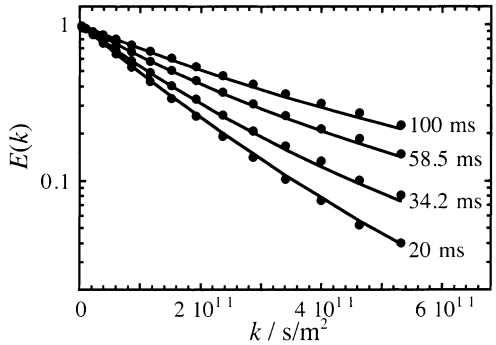

Figure 6. Echo attenuation curves $E(k)$ from a potato starch sample hydrated to 0.26 g water/g solid. The values of the diffusion time t are indicated in the figure. Circles, experimental; lines, fit of eq 8 with $\exp(-kD)$ replaced by eq 3 and $P_D(D)$ calculated with eq 7 using $P_\theta(\theta)$ for a 3D powder.

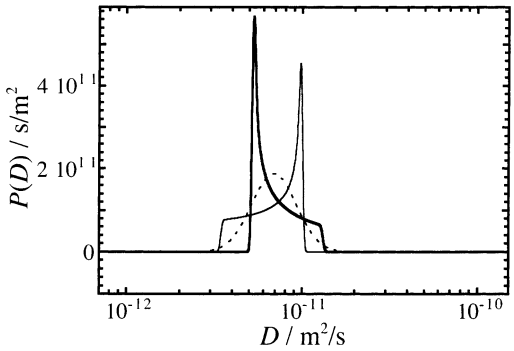

Figure 7. Distributions of diffusion coefficients $P_D(D)$ that satisfy the data in Figure 6. Thick solid line, 3D powder with $D_\parallel > D_\perp$; thin solid line, 3D powder with $D_\parallel < D_\perp$; and thin dashed line, log-normal distribution.

Hills et al.[10] discussed several different ways to analyze water diffusion data obtained on a packed bed of starch granules using the PFG STE technique. In conclusion, the absence of a diffusion time dependence favors a model with unbounded diffusion in a lower dimensional space. A model with 1D and 2D diffusion, corresponding to a 3D powder of anisotropic domains with either $D_\perp$ or $D_\parallel$ equal to zero in the terminology of this paper, was proposed as the most likely model. Hills et al. found that the diffusion data obtained at a water content of 0.30 g water/g total falls between the 1D and 2D models. Notably, they did not detect any diffusion time dependence due to cross relaxation although the PFG STE technique was used. The reason for this might be that the experiments were performed at a rather low proton resonance frequency of 22 MHz. Furthermore, Callaghan[8] found that 1D diffusion was in agreement with data obtained with PFG SE experiments on wheat starch hydrated at 90% relative humidity.

Echo attenuation curves obtained on the potato starch sample at a water content of 0.26 g water/g starch are displayed in Figure 6. The apparent dependence on t is an effect of cross relaxation.[30] The facts presented above make it likely that the data can be analyzed with a 3D powder distribution of anisotropic domains where $D_\perp$ and $D_\parallel$ are comparable in magnitude. In Figure 7, we display three distributions that give an equally good fit to the experimental data in Figure 6. One

TABLE 2: Moments of the Distributions in Figure 7

	$\langle D\rangle$/ $(10^{-12}$ m^2/s)	$\langle D^2\rangle$/ $(10^{-12}$ m^2/s$)^2$	$\langle D^3\rangle$/ $(10^{-12}$ m^2/s$)^3$
3D powder $D_\parallel > D_\perp$	7.91	5.7	8.5
3D powder $D_\parallel < D_\perp$	7.84	3.9	−5.0
log−normal	7.85	5.6	13

important feature is that the distributions are rather narrow as compared to the results obtained on cellulose. On account of the small difference between $D_\perp$ and $D_\parallel$, it cannot be decided which one is the largest. The two cases $D_\parallel > D_\perp$ and $D_\parallel < D_\perp$ give equally good fits to the experimental data. A Monte Carlo error analysis of the data evaluated with the 3D powder distribution and assuming that $D_\parallel > D_\perp$, which is the case for wheat starch,[8] yields the results $\langle D\rangle = (7.8\pm0.1) \times 10^{-12}$ m^2/s and $D_\parallel/D_\perp = 2.5 \pm 0.3$ with 67% confidence level. The moments of the three distributions are presented in Table 2. Also in this case, $\langle D\rangle$ can be estimated with any reasonable model.

Conclusions

We have presented a way to calculate echo attenuation curves for powder distributions of anisotropic domains when cross relaxation effects on the result of the stimulated echo experiment are important. The anisotropy of cellulose and starch with respect to water diffusion was estimated using models in agreement with the known supermolecular organization and domain orientation. It was shown that the orientation averaged diffusion coefficient can be obtained with the assumption of a log−normal distribution, although this distribution is not physically correct.

Acknowledgment. This work was financially supported by the Colloid and Interface Technology program of the Swedish Foundation for Strategic Research (SSF).

References and Notes

(1) Callaghan, P. T. *Principles of nuclear magnetic resonance microscopy*, 1st ed.; Oxford University Press: Oxford, U.K., 1991.
(2) Price, W. S. *Concepts Magn. Reson.* **1997**, *9*, 299−336.
(3) Kimmich, R. *NMR: tomography, diffusometry, relaxometry*, 1st ed.; Springer-Verlag: Berlin, Germany, 1997.
(4) Stallmach, F.; Kärger, J. *Adsorption* **1999**, *5*, 117−133.
(5) Callaghan, P. T.; Söderman, O. *J. Phys. Chem.* **1983**, *87*, 1737−1744.
(6) Joabsson, F.; Nydén, M.; Linse, P.; Söderman, O. *J. Phys. Chem. B* **1997**, *101*, 9710−9716.
(7) Gaemers, S.; Bax, A. *J. Am. Chem. Soc.* **2001**, *123*, 12343−12352.
(8) Callaghan, P. T.; Jolley, K. W.; Lelievre, J. *Biophys. J.* **1979**, *28*, 133−141.
(9) Tang, H.-R.; Godward, J.; Hills, B. *Carbohydr. Polym.* **2000**, *43*, 375−387.
(10) Hills, B. P.; Godward, J.; Manning, C. E.; Biechlin, J. L.; Wright, K. M. *Magn. Reson. Imaging* **1998**, *16*, 557−564.
(11) MacGregor, R. P.; Peemoeller, H.; Schneider, M. H.; Sharp, A. R. *J. Appl. Polym. Sci.: Appl. Polym. Symp.* **1983**, *37*, 901−909.
(12) Li, T.-Q.; Henriksson, U.; Klason, T.; Ödberg, L. *J. Colloid Interface Sci.* **1992**, *154*, 305−315.
(13) Peschier, L. J. C.; Bouwstra, J. A.; de Bleyser, J.; Junginger, H. E.; Leyte, J. C. *J. Magn. Reson. B* **1996**, *110*, 150−157.
(14) Topgaard, D.; Söderman, O. *Langmuir* **2001**, *17*, 2694−2702.
(15) Stejskal, E. O.; Tanner, J. E. *J. Chem. Phys.* **1965**, *42*, 288−292.
(16) Jakes, J. *Collect. Czech. Chem. Commun.* **1995**, *60*, 1781−1797.
(17) Whittal, K. P.; MacKay, A. L. *J. Magn. Reson.* **1989**, *84*, 134−152.
(18) Overloop, K.; Van Gerven, L. *J. Magn. Reson.* **1992**, *100*, 303−315.
(19) Bear, J. *Dynamics of fluids in porous media*; Dover Publications: New York, 1988.
(20) Hartley, I. D.; Kamke, F. A.; Peemoeller, H. *Holzforschung* **1994**, *48*, 474−479.
(21) Tanner, J. E. *J. Chem. Phys.* **1970**, *52*, 2523−2526.
(22) Fauth, J.; Schweiger, A.; Braunschweiler, L.; Forrer, J.; Ernst, R. R. *J. Magn. Reson.* **1986**, *66*, 74−85.
(23) Goldman, M.; Shen, L. *Phys. Rev.* **1966**, *144*, 321−331.
(24) Johnson, C. S., Jr. Transport ordered 2D-NMR spectroscopy. In *Nuclear magnetic resonance probes of molecular dynamics*; Tycko, R., Ed.; Kluwer Academic Publishers: Dordrecht, The Netherlands, 1994; pp 455−488.
(25) Fengel, D.; Wegener, G. *Wood: chemistry, ultrastructure and reactions*; Walter de Gruyter: New York, 1984.
(26) Alper, J. S.; Gelb, R. I. *J. Phys. Chem.* **1990**, *94*, 4747−4751.
(27) Provencher, S. W. *Comput. Phys. Commun.* **1982**, *27*, 213−227.
(28) Provencher, S. W. *Comput. Phys. Commun.* **1982**, *27*, 229−242.
(29) Gallant, D. J.; Bouchet, B.; Baldwin, P. M. *Carbohydr. Polym.* **1997**, *32*, 177−191.
(30) Topgaard, D.; Söderman, O. *Prog. Colloid Polym. Sci.* **2002**, *120*, 47−51.